Mon. Not. R. Astron. Soc. **000**, 1–5 (2011) Printed 30 December 2014 (MN LATEX style file v2.2)

# Astrochemistry at work in the L1157–B1 shock: acetaldehyde formation

C. Codella[1]*, F. Fontani[1], C. Ceccarelli[2,3], L. Podio[1], S. Viti[4], R. Bachiller[5], M. Benedettini[6], B. Lefloch[2,3]

[1] *INAF-Osservatorio Astrofisico di Arcetri, L.go E. Fermi 5, Firenze, 50125, Italy*
[2] *Univ. Grenoble Alpes, IPAG, F-38000 Grenoble, France*
[3] *CNRS, IPAG, F-38000 Grenoble, France*
[4] *Department of Physics and Astronomy, University College London, Gower Str eet, London, WC1E 6BT, UK*
[5] *IGN, Observatorio Astronómico Nacional, Calle Alfonso XIII, 28004 Madrid, Spain*
[6] *INAF, Istituto di Astrofisica e Planetologia Spaziali, via Fosso del Cavaliere 100, 00133 Roma, Italy*

arXiv:1412.8318v1 [astro-ph.EP] 29 Dec 2014

Accepted date. Received date; in original form date

**ABSTRACT**

The formation of complex organic molecules (COMs) in protostellar environments is a hotly debated topic. In particular, the relative importance of the gas phase processes as compared to a direct formation of COMs on the dust grain surfaces is so far unknown. We report here the first high-resolution images of acetaldehyde ($CH_3CHO$) emission towards the chemically rich protostellar shock L1157-B1, obtained at 2 mm with the IRAM Plateau de Bure interferometer. Six blueshifted $CH_3CHO$ lines with $E_u$ = 26-35 K have been detected. The acetaldehyde spatial distribution follows the young ($\sim$ 2000 yr) outflow cavity produced by the impact of the jet with the ambient medium, indicating that this COM is closely associated with the region enriched by iced species evaporated from dust mantles and released into the gas phase. A high $CH_3CHO$ relative abundance, 2–3 $\times$ $10^{-8}$, is inferred, similarly to what found in hot-corinos. Astrochemical modelling indicates that gas phase reactions can produce the observed quantity of acetaldehyde only if a large fraction of carbon, of the order of 0.1%, is locked into iced hydrocarbons.

**Key words:** Molecular data – Stars: formation – radio lines: ISM – submillimetre: ISM – ISM: molecules

## 1 INTRODUCTION

Complex organic molecules (COMs) have a key role among the many molecules so far detected in space: since they follow the same chemical rules of carbon-based chemistry, which terrestrial life is based on, they may give us an insight into the universality of life. Of course, large biotic molecules are not detectable in space, certainly not via (sub)millimeter observations. However, to determine whether pre-biotic molecules may form in space, we first need to understand the basic mechanisms that form smaller COMs. There is an extensive literature on the subject and still much debate on how COMs may form in space (e.g. Herbst & van Dishoeck 2009; Caselli & Ceccarelli 2012; Bergin 2013). Two basic processes are, in principle, possible: COMs may form on the grain surfaces or in gas phase. It is possible and even probable that the two processes are both important in different conditions for different molecules.

Acetaldehyde ($CH_3CHO$) has been detected in a large range of interstellar conditions and with different abundances, namely in hot cores (Blake et al. 1986), hot corinos (Cazaux et al. 2003), cold envelopes (Jaber et al. 2014), Galactic Center clouds (Requena-Torres et al. 2006) and pre-stellar cores (Öberg et al. 2010). Grain surface models predict that $CH_3CHO$ is one of the simplest COMs and can be formed either by the combination of two radicals on the grain surface, $CH_3$ and HCO, which become mobile when the grain temperature reaches $\sim$30 K (Garrods & Herbst 2006), or by irradiation of iced $CH_4$, $CO_2$ and other iced species (Bennett et al. 2005). For the former route, the two radicals are predicted to be formed either because of the photolysis of more complex molecules on the grain mantles or, more simply, because of the partial hydrogenation of simple biatomic molecules on the grain mantles (Taquet et al.

* E-mail: codella@arcetri.astro.it

© 2011 RAS

2012). Conversely, gas phase models claim that acetaldehyde is easily formed by the oxidation of hydrocarbons, which are produced by the hydrogenation of carbon chain on the grain mantles (Charnley et al. 1992, 2004). Finally, a further possible mechanism involving formation in the very high density gas-phase immediately after ice mantles are sublimated has been proposed by Rawlings et al. (2013).

In general, it is very difficult to distinguish which of these three mechanisms are at work and, consequently, their relative importance. The chemically rich shocked region L1157-B1 offers a unique possibility to test these theories, as it is a place where the dust is not heated by the protostar, but some of the grain mantles are sputtered/injected in the gas phase because of the passage of a shock (see e.g. Fontani et al. 2014). The L1157-mm protostar ($d$ = 250 pc) drives a chemically rich outflow (Bachiller et al. 2001), associated with molecular clumpy cavities (Gueth et al. 1996), created by episodic events in a precessing jet. Located at the apex of the more recent cavity, the bright bow shock called B1 has a kinematical age of 2000 years. This shock spot has been the target of several studies (e.g. the Large Programs Herschel/CHESS[1] (Chemical Herschel Surveys of Star forming regions; Ceccarelli et al. 2010; and IRAM-30m/ASAI[2] (Astrochemical Survey At IRAM). In this Letter we report high spatial resolution observations of acetaldehyde, with the aim to constrain and quantify the contribution of gas phase chemistry to the $CH_3CHO$ formation.

## 2 OBSERVATIONS

L1157-B1 was observed with the IRAM Plateau de Bure (PdB) 6-element array in April–May 2013 using both the C and D configurations, with 21–176 m baselines, filtering out structures $\geqslant 20''$, and providing an angular resolution of $2''.5 \times 2''.3$ (PA = 90°). The primary HPBW is $\sim 37''$. The observed $CH_3CHO$ lines (see Table 1) at $\sim$ 134–136 GHz were detected using the WideX backend which covers a 4 GHz spectral window at a 2 MHz ($\sim$ 4.4 km s$^{-1}$) spectral resolution. The system temperature was 100–200 K in all tracks, and the amount of precipitable water vapor was generally $\sim$ 5 mm. Calibration was carried out following standard procedures, using GILDAS-CLIC[3]. Calibration was performed on 3C279 (bandpass), 1926+611, and 1928+738 (phase and amplitude). The absolute flux scale was set by observing MWC349 ($\sim$ 1.5 Jy at 134 GHz). The typical rms noise in the 2 MHz channels was $\sim$ 0.7 mJy beam$^{-1}$.

## 3 RESULTS: IMAGES AND SPECTRA

Acetaldehyde emission has been clearly (S/N $\geqslant$ 10) detected towards L1157–B1. Fig. 1 shows the map of the $CH_3CHO(7_{0,7}–6_{0,6})$ E and A lines integrated emission. In order to verify whether the present $CH_3CHO$ image is altered by filtering of large-scale emission, we produced the $CH_3CHO(7_{0,7}–6_{0,6})$ E+A spectrum summing the emission measured at PdBI in a circle of diameter equal to the half-power beam width (HPBW) of the IRAM-30m telescope ($17''$). We evaluated the missing flux by comparing such emission with the spectrum directly measured with the single-dish (from the ASAI spectral survey, Lefloch et al., in preparation). As already found for HDCO by Fontani et al. (2014), with the PdBI we recover more than 80% of the flux, indicating that both tracers do not have significant extended structures. The spatial distribution reported in Fig. 1 shows that $CH_3CHO$ is mainly associated with two regions: (i) the eastern B0-B1 cavity opened by the precessing jet (called 'E-wall', see Fig. 1 in Fontani et al. 2014), and (ii) the arch-like structure composed by the B1a-e-f-b clumps identified by $CH_3CN$ (called 'arch'). The red, turquoise, and magenta polygons shown in Fig. 1 sketch out these two regions, intersecting at the position of the B1a clump. Note that B1a is in turn located where the precessing jet is expected to impact the cavity producing a dissociative J-shock (traced by high velocity SiO, $H_2O$, [FeII], [OI], and high-J CO emission: e.g. Gueth et al. 1998, Benedettini et al. 2012).

**Table 1.** List of $CH_3CHO$ transitions detected towards L1157-B1

| Transition | $\nu^{a}$ (GHz) | $E_{u}{}^{a}$ (K) | $S\mu^{2a}$ (D$^2$) | log(A/s$^{-1}$)$^{a}$ |
|---|---|---|---|---|
| $(7_{0,7}–6_{0,6})$E | 133.830 | 26 | 88.5 | –4.04 |
| $(7_{0,7}–6_{0,6})$A | 133.854 | 26 | 88.4 | –4.08 |
| $(7_{2,6}–6_{2,5})$A | 134.694 | 35 | 81.3 | –4.11 |
| $(7_{2,6}–6_{2,5})$E | 134.895 | 35 | 79.7 | –4.12 |
| $(7_{2,5}–6_{2,4})$E | 135.477 | 35 | 79.7 | –4.11 |
| $(7_{2,5}–6_{2,4})$A | 135.685 | 35 | 81.3 | –4.10 |

[a] From the Jet Propulsion Laboratory database (Pickett et al. 1998).

Figure 2 shows the $CH_3CHO$ line spectrum observed with the 3.6 GHz WideX bandwidth towards the brightest clump, B1a. Up to six lines ($E_u$ = 26–35 K, see Table 1) are detected with a S/N > 3. Using the GILDAS–Weeds package (Maret et al. 2011) and assuming optically thin emission and LTE conditions, we produced the synthetic spectrum (red line in Fig. 2) that best fits the observed one. Note that the $CH_3CHO$ lines are blue-shifted, by 2 km s$^{-1}$, with respect to the cloud systemic velocity (+2.6 km s$^{-1}$: Bachiller & Peréz Gutiérrez 1997), and have linewidths of 8 km s$^{-1}$. Similarly, we extracted the $CH_3CHO$ line spectrum towards the three B1 zones, 'E-wall', 'arch', and 'head', shown in Fig. 1. Table 2 reports the measured peak velocities, intensities (in $T_B$ scale), FWHM linewidths, and integrated intensities, for each of the three zones.

## 4 $CH_3CHO$ ABUNDANCE

Figure 1 compares the $CH_3CHO$ distribution with that of HDCO (Fontani et al. 2014), showing an excellent agreement, with weak or no emission at the head of the bow B1 structure (called 'head'). The acetaldehyde emission is concentrated towards the 'E-wall' and 'arch' zones, namely the part of B1 associated with the most recent shocked material, as probed by the HDCO emission. This is further supported by the fact that the brightest acetaldehyde emission comes where also $CH_3OH$, another dust mantle product, and $CH_3CN$, a 6-atoms COM, emission peak (Codella

[1] http://www-laog.obs.ujf-grenoble.fr/heberges/chess/
[2] http://www.oan.es/asai
[3] http://www.iram.fr/IRAMFR/GILDAS

**Table 2.** Observed parameters (in $T_{\rm B}$ scale) of the $CH_3CHO(7_{0,7}–6_{0,6})$E and A emission, and acetaldehyde column densities $N_{\rm CH_3CHO}$ derived in the 3 regions identified in Fig. 1 (E-wall, arch, and head) following Fontani et al. (2014), see Sect. 3. The (range of) excitation temperatures ($T_{\rm ex}$) used to derive $N_{\rm CH_3CHO}$ have been assumed equal to the rotation temperatures derived in Codella et al. (2012), Lefloch et al. (2012), and Fontani et al. (2014). The last columns report the $X(CH_3CHO)/X(CH_3OH)$ and $X(CH_3CHO)/X(HDCO)$ abundance ratios using the $CH_3OH$ and HDCO data (and similar beams) by Benedettini et al. (2013) and Fontani et al. (2014).

| Transition | $T_{\rm peak}$[a] (mK) | $V_{\rm peak}$[a] (km s$^{-1}$) | $FWHM$[a] (km s$^{-1}$) | $F_{\rm int}$[a] (mK km s$^{-1}$) | $N_{\rm CH_3CHO}$[b] ($10^{12}$ cm$^{-2}$) 10 K – 70 K | $\rm CH_3CHO/CH_3OH$ ($10^{-2}$) 10 K – 70 K | $\rm CH_3CHO/HDCO$ 10 K – 70 K |
|---|---|---|---|---|---|---|---|
| | | | | E-wall | | | |
| $7_{0,7}–6_{0,6}$ E | 30(3) | +0.4(0.4) | 8.2(1.0) | 264(28) | 5.0(0.3)–9.2(0.5) | 1.7(0.1)–11.0(0.6) | 1.9(0.2)–0.9(0.1) |
| $7_{0,7}–6_{0,6}$ A | 29(3) | +0.5(0.5) | 8.6(1.3) | 263(31) | | | |
| | | | | Arch | | | |
| $7_{0,7}–6_{0,6}$ E | 71(7) | –0.9(0.3) | 9.2(0.8) | 748(54) | 15.9(0.1)–29.4(0.1) | 0.6(0.1)–4.2(0.1) | 7.6(1.1)–3.7(0.5) |
| $7_{0,7}–6_{0,6}$ A | 76(7) | –0.2(0.9) | 8.0(0.5) | 608(42) | | | |
| | | | | Head | | | |
| $7_{0,7}–6_{0,6}$ E | 14(3) | +0.9(0.5) | 8.0(1.1) | 81(13) | 1.7(0.3)–3.1(0.5) | 0.2(0.1)–0.7(0.1) | $\geqslant 1.5$ |
| $7_{0,7}–6_{0,6}$ A | 13(3) | +0.9(0.6) | 5.2(1.6) | 81(13) | | | |

[a] The errors are the gaussian fit uncertainties. The spectral resolution is 4.4 km s$^{-1}$. [b] Derived using the $(7_{0,7}–6_{0,6})$ E and A emissions.

et al. 2009, Benedettini et al. 2013). Finally, the $CH_3CHO$ observed emission is also confined in the low-velocity range ($FWHM \sim 8$ km s$^{-1}$) of the L1157-B1 outflow, which is dominated by the extended B1 bow-cavity, according to Lefloch et al. (2012) and Busquet et al. (2014). In summary, similarly to HDCO, $CH_3CHO$ traces the extended interface between the shock and the ambient gas, which is chemically enriched by the sputtering of the dust mantles.

To derive the column density, we used the LTE populated and optically thin assumption and best fitted the six detected lines of Tables 1–2. Towards the B1a peak, we find $N_{\rm CH_3CHO} = 9 \times 10^{13}$ cm$^{-2}$, and a rotational temperature of $T_{\rm rot} = 15$ K, in agreement with the value derived for the molecular cavity from single-dish CO and HDCO measurements (10–70 K; Lefloch et al. 2012, Codella et al. 2012). Assuming rotational temperatures between 10 and 70 K (Table 2) we derived a column density of 5–30 $\times 10^{12}$ cm$^{-2}$ in the 'E-wall' and 'arch' regions, and $\sim$ 2–3 $10^{12}$ cm$^{-2}$ in the 'head'. The size of the regions (at $3\sigma$ level) is $9''$ ('E-wall'), $7''$ ('arch'), and $8''$ ('head'). An estimate of the $CH_3CHO$ abundance can be derived using the the CO column density $\simeq 10^{17}$ cm$^{-2}$ derived by Lefloch et al. (2012) on a $20''$ scale. We derived $N_{\rm CH_3CHO}$ using the $CH_3CHO$ spectrum extracted on the same scale and assuming 10–70 K. We find $N_{\rm CH_3CHO} \sim 0.9–1.6 \times 10^{13}$ cm$^{-2}$, which implies a high abundance, $X(\rm CH_3CHO) \simeq 2–3 \times 10^{-8}$, similar to what has been measured in hot-corinos ($\simeq 2–6 \times 10^{-8}$, Cazaux et al. 2003), and larger than that measured in prestellar cores ($\sim 10^{-11}$, Vastel et al. 2014) and towards high-mass star forming regions ($\sim 10^{-11}$–$10^{-9}$, Cazaux et al. 2003; Charnley 2004).

## 5 GAS PHASE FORMATION OF $CH_3CHO$

The ratio between $N_{\rm CH_3CHO}$ and the column density of HDCO, i.e. a molecule which in L1157-B1 is predominantly released by grain mantles (Fontani et al. 2014), is higher (even if we consider the uncertainties, see Table 2) in the 'arch' with respect to the 'E-wall' by a factor $\sim$ 2–8. Assuming the same grain mantle composition and release mechanism, this difference suggests that, in the 'arch', a significative fraction of the observed $CH_3CHO$ is formed in the gas phase. In the gas phase, the injection from grain mantles of ethane ($C_2H_6$) is expected to drive first $C_2H_5$ and successively acetaldehyde (e.g. Charnley 2004; Vasyunin & Herbst 2013): the overlap between the HDCO (Fontani et al. 2014) and $CH_3CHO$ emitting regions supports this scenario. We can, therefore, use the measured $CH_3CHO$ abundance to constrain the quantity of $C_2H_5$ that has to be present in the gas phase in order to produce the observed quantity of $CH_3CHO$. To this end, we use the chemical code ASTROCHEM[4], a pseudo time dependent model that follows the evolution of a gas cloud with a fixed temperature and density considering a network of chemical reactions in the gas phase. We followed the same 2-steps procedure adopted in Podio et al. (2014) and Mendoza et al. (2014), to first compute the steady-state abundances in the cloud (i.e. $\rm T_{kin}$=10 K, $\rm n_{H_2}$=$10^4$ cm$^{-3}$, $\zeta$=3 $10^{16}$ s$^{-1}$); and then we follow the gas evolution over 2000 yr at the shocked conditions (i.e. $\rm T_{kin}$=70 K and $\rm n_{H_2}$=$10^5$ cm$^{-3}$). To estimate the influence of a possibly larger gas $\rm T_{kin}$ during the passage of the shock, we also run cases with temperatures up to 1000 K. We adopt the OSU[5] chemical network and assume visual extinction of $\rm A_V = 10$ mag and grain size of 0.1 $\mu$m. We assume that the abundances of OCS and $CO_2$ are also enhanced by the passage of the shock, namely their abundance in step 2 is $X(\rm CO_2) = 6\ 10^{-5}$ and $X(\rm OCS) = 6\ 10^{-6}$. Similarly, we assume that the abundance of methanol in step 2 is $2\ 10^{-6}$, in agreement with the most recent determination in L1157-B1 by Mendoza et al. (2014). Finally, we varied the $C_2H_5$ abundance from $2 \times 10^{-7}$ to $2 \times 10^{-5}$. As expected, the predicted steady-state abundance of acetaldehyde in the cloud is very low ($1.5\ 10^{-15}$). However, once $C_2H_5$ is in the gas phase, it rapidly reacts with oxygen forming abundant acetaldehyde on timescale shorter than 100 years (Fig. 3). The $CH_3CHO$ abundance reaches the observed value, $\simeq 2–3 \times 10^{-8}$, at the shock age (2000 years), for $C_2H_5 \sim 2–6 \times 10^{-7}$. Note that

[4] http://smaret.github.io/astrochem/
[5] http://faculty.virginia.edu/ericherb

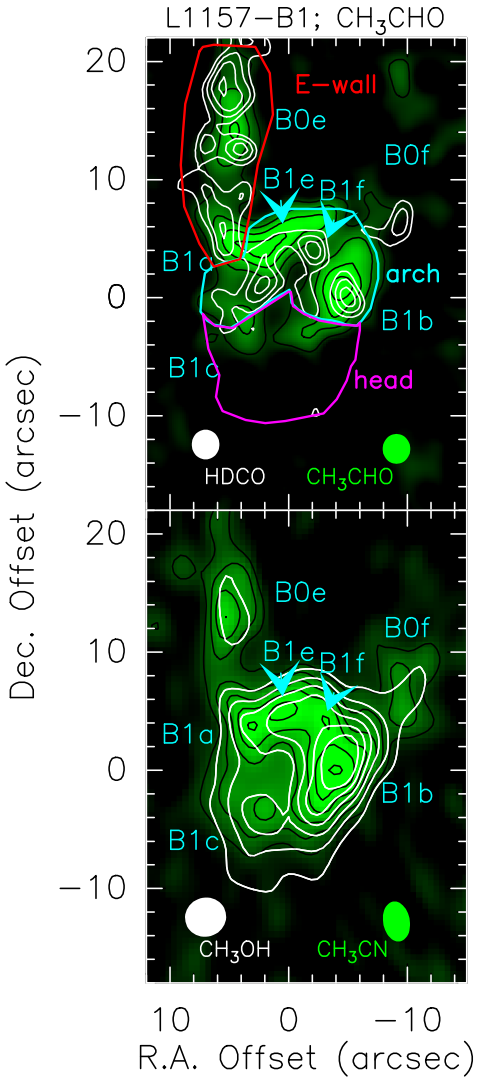


**Figure 1.** Chemical differentation in L1157–B1: the maps are centred at: $\alpha$(J2000) = $20^h$ $39^m$ $09\overset{s}{.}5$, $\delta$(J2000) = +68° 01′ 10″.0, i.e. at $\Delta\alpha$ = +21″.7 and $\Delta\delta$ = –64″.0 from the driving protostar. *Upper panel:* $CH_3CHO(7_{0,7}–6_{0,6})$E+A integrated emission (green colour, black contours) on top of the HDCO($2_{1,1}$ − $1_{0,1}$) line (white contours; Fontani et al. 2014). First contour and steps of the $CH_3CHO$ image correspondes to 3$\sigma$ (1 mJy beam $^{-1}$). The ellipses show the synthesised HPBW (2″.5 × 2″.3, PA = 90°). The red, turquoise, and magenta polygons called 'E-wall', 'arch', and 'head' indicate the 3 portions of L1157-B1 selected by Fontani et al. (2014) to investigate $H_2CO$ deuteration. *Bottom panel:* $CH_3CN(8_K–7_K)$ emission (green colour, black contours; Codella et al. 2009) on top of the $CH_3OH(3_2–2_K)$ emission (white; Benedettini et al. 2013). The HPBWs are: 3″.4 × 2″.1 (PA = 10°) for $CH_3CN$ and 3″.5 × 2″.3 (PA = 12°) for $CH_3OH$. The labels indicate the L1157-B1 clumps identified using the $CH_3CN$ image (Codella et al. 2009).

we obtain the same result if the gas temperature is $\leqslant$ 500 K, and a 30% higher value at 1000 K. Figure 3 shows also that the $CH_3CHO/CH_3OH$ abundance ratio is expected to drop between $10^3$ yr and $10^4$ yr. A different age could, therefore, justify the slightly smaller $CH_3CHO/CH_3OH$ ratio observed towards the 'head' region.

## 6 DISCUSSION AND CONCLUSIONS

We have shown that acetaldehyde is abundant, $X(CH_3CHO) \simeq 2–3 \times 10^{-8}$, in the gas associated with the passage of a shock and enriched by iced species sputtered from grain mantles and injected into the gas phase. The measured acetaldehyde abundance could be consistent with the scenario of oxydation of gaseous hydrocarbons formed in a previous phase and released by the grain mantles. However, the abundance of the $C_2H_5$ required to reproduce the measured $CH_3CHO$ is very high, $\sim$ 2–6 × $10^{-7}$, namely less than 0.6% the elemental gaseous carbon. There are no observations of $C_2H_5$, hence it is impossible to compare with direct estimates of the abundance of this molecule. However, it has been argued that large quantities of frozen methane, of a few % of iced mantle water, is found around the L1527-mm protostar, where the detection of $CH_3D$ (Sakai et al. 2012) indicates $X(CH_4) \simeq$ 0.4–1.5 × $10^{-5}$. This large abundance has been attributed to a low density of the pre-collapse core from which L1527-mm originated (Aikawa et al. 2008). Interestingly, the analysis of the deuteration of water, methanol and formaldehyde in L1157-B1 led Codella et al. (2012) to conclude that also the mantles of L1157-B1 were formed in relatively low density ($\sim 10^3$ cm$^{-3}$) conditions.

To conclude, in the specific case of L1157-B1, gas phase reactions can produce the observed quantity of acetaldehyde only if a large fraction of carbon, of the order of 0.1%, is locked into iced hydrocarbons. Further observations of the hydrocarbons abundance in L1557-B1 are needed to confirm or dismiss our hypothesis.

## ACKNOWLEDGMENTS

The authors are grateful to P. Caselli for instructive comments and suggestions, as well as to the IRAM staff for its help in the calibration of the PdBI data. This research has received funding from the European Commission Seventh Framework Programme (FP/2007-2013, n. 283393, RadioNet3), the PRIN INAF 2012 – JEDI, and the Italian Ministero dell'Istruzione, Università e Ricerca through the grant Progetti Premiali 2012 – iALMA. LP has received funding from the European Union Seventh Framework Programme (FP7/2007-2013, n. 267251). CC and BL acknowledge the financial support from the French Space Agency CNES, and RB from Spanish MINECO (FIS2012-32096).

## REFERENCES

Aikawa Y., Wakelam V., Garrod R.T., & Herbst E. 2008, ApJ 674, 993
Bachiller R., & Peréz Gutiérrez M. 1997, ApJ 487, L93
Benedettini, M., Busquet, B., Lefloch, B., et al. 2012, A&A 539, L3
Bennett C.J., Osamira Y., Lebar M.D., & KAiser R.I. 2005, ApJ 634, 968
Bergin, E.A. 2013, XVII Special Courses at the National Observatory of Rio de Janeiro. AIP Conference Proceedings, arXiv:1309.4729
Blake G.A., Masson C.R., Phillips T.G., & Sutton E.C. 1986, ApJS 60, 357

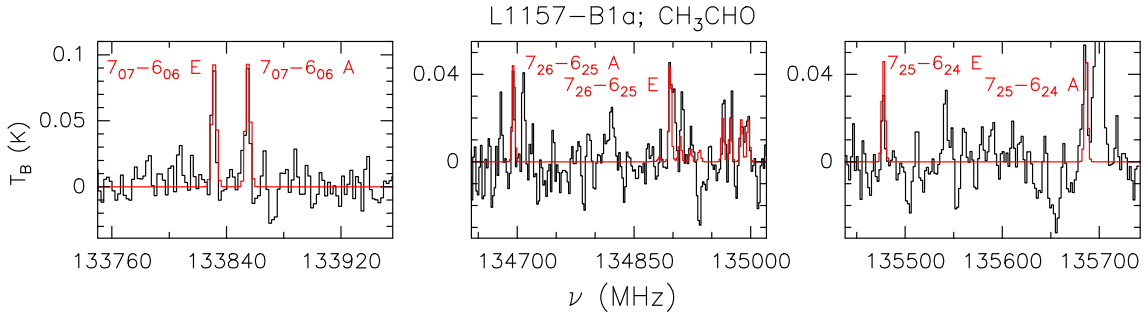


**Figure 2.** $CH_3CHO$ emission (in $T_B$ scale) extracted at the B1a position ($\alpha$(J2000) = $20^h$ $39^m$ $10\overset{s}{.}2$, $\delta$(J2000) = +68° 01′ 12″.0). the three panels show the frequency intervals of the 4 GHz wide WideX where the six $CH_3CHO$ lines with S/N $\geqslant 3\sigma$ (33 mK) are located (see Table 1). The red line shows the synthetic spectra which better reproduce the observations: it has been obtained with the GILDAS–Weeds package (Maret et al. 2011) assuming optically thin emission and LTE conditions with $N_{CH_3CHO} = 9 \times 10^{13}$ cm$^{-2}$, $T_{ex} = 15$ K, $v_{LSR} = +0.6$ km s$^{-1}$, and FWHM linewidth = 8.0 km s$^{-1}$.

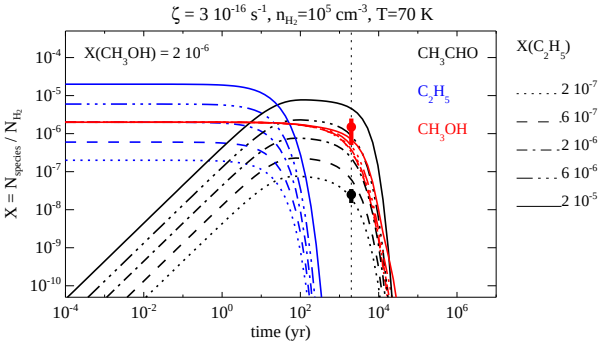


**Figure 3.** Evolution of acetaldehyde ($CH_3CHO$, black), ($C_2H_5$, blue), and methanol ($CH_3OH$, red) abundances in the shock as a function of time. Observed abundances (colour circles) are overplotted at the shock age ($t_{shock} \sim 2000$ years, vertical dotted line). The evolution is computed from steady-state values in the cloud ($n_{H_2} = 10^4$ cm$^{-3}$, $T_{kin} = 10$ K, $\zeta = 3 \times 10^{-16}$ s$^{-1}$) by enhancing the gas temperature and density ($n_{H_2} = 10^5$ cm$^{-3}$, $T_{kin} = 70$ K), and the abundance of molecules which are thought to be sputtered off dust grain mantles. We set $X_{CO_2} = 6 \times 10^{-5}$ and $X_{OCS} = 6 \times 10^{-6}$ as in Podio et al. 2014, $X_{CH_3OH} = 2 \times 10^{-6}$ (Mendoza et al. 2014), and vary the abundance of $C_2H_5$ between $2 \times 10^{-7}$ and $2 \times 10^{-5}$.


Busquet G., Lefloch B., Benedettini, M., et al. 2014, A&A 561, 120

Benedettini, M., Viti, S., Codella, C., et al. 2013, MNRAS 436, 179

Caselli, P. & Ceccarelli, C. 2012, A&ARv, 20, 56

Cazaux S., Tielens A.G.G.M., Ceccarelli C., et al. 2003, ApJ 593, L51

Ceccarelli C., Bacmann A., Boogert A., et al. 2010, A&A 521, L22

Charnley S.B., 2004, Adv. Space Res. 33, 23

Charnley S.B., Tielens A.G.G.M., & Millar T.J. 1992, ApJ 399, L71

Codella C., Benedettini M., Beltrán M.T., et al. 2009, A&A 507, L25

Codella C., Ceccarelli C., Lefloch B., et al. 2012, ApJ, 757, L9

Fontani F., Codella C., Ceccarelli C., et al. 2014, ApJ 788, L43

Garrod R.T., & Herbst E. 2006, A&A 457, 927

Garrod R.T., Wakelam V., & Herbst E. 2007, A&A 467, 1103

Garrod R.T., Weaver S.L.W., & Herbst E. 2008, ApJ 682, 283

Garrod R.T., Vasyunin A.I., Semenov D.A., Wiebe D.S., & Henning Th. 2009, ApJ 700, L43

Gueth F., Guilloteau S., & Bachiller R. 1996, A&A 307, 891

Gueth F., Guilloteau S., & Bachiller R. 1998, A&A 333, 287

Herbst E., & van Dishoeck E.F. 2009, ARA&A 47, 427

Jaber A.A., Ceccarelli C., Kahane C., & Caux E. 2014, ApJ 791, 29

Lefloch B., Cabrit S., Busquet G., et al. 2012, ApJ, 757, L25

Maret S., Hily-Blant P., Pety J., et al., A&A 526, A47

Öberg K.I., Bottinelli S., Jørgensen J.K., van Dishoeck E.F. 2010, ApJ 716, 825

Occhiogrosso A., Vasyunin A., Herbst E., et al. 2014, A&A 564, 123

Pickett H.M., Poynter R.L., Cohen E.A., et al. 1998, J. Quant. Spectrosc. & Rad. Transfer 60, 883

Podio L., Lefloch B., Ceccarelli C., Codella C., & Bachiller R. 2014, A&A 565, 64

Requena-Torres M.A.; Martín-Pintado J., Rodríguez-Franco A., et al. 2006, A&A 455, 971

Rawlings J.M.C., Williams D.A., Viti S., & Cecchi-Pestellini C. 2013, MNRAS 430, 264

Sakai N., Shirley Y.L., Sakai T., et al. 2012, ApJ 758, L4

Taquet, V., Ceccarelli, C., & Kahane, C. 2012, ApJ 784, L3

Vastel C., Ceccarelli C., Lefloch B., & Bachiller R. 2014, ApJ 795, L2

Vasyunin A.I., & Herbst E. 2013, ApJ 769, 34


This paper has been typeset from a TEX/ LATEX file prepared by the author.